# Accepted Manuscript

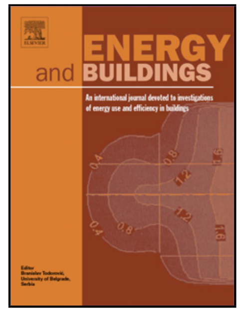


Title: A computational multi-objective optimization method to improve energy efficiency and thermal comfort in dwellings

Author: Facundo Bre Víctor D. Fachinotti

| | |
|---|---|
| PII: | S0378-7788(17)31804-2 |
| DOI: | http://dx.doi.org/doi:10.1016/j.enbuild.2017.08.002 |
| Reference: | ENB 7831 |

| | |
|---|---|
| To appear in: | *ENB* |

| | |
|---|---|
| Received date: | 22-5-2017 |
| Revised date: | 5-7-2017 |
| Accepted date: | 2-8-2017 |

Please cite this article as: Facundo Bre, Víctor D. Fachinotti, A computational multi-objective optimization method to improve energy efficiency and thermal comfort in dwellings, *<![CDATA[Energy & Buildings]]>* (2017), http://dx.doi.org/10.1016/j.enbuild.2017.08.002

# A computational multi-objective optimization method to improve energy efficiency and thermal comfort in dwellings

Facundo Bre[a,b], Víctor D. Fachinotti[a]

[a] Centro de Investigación de Métodos Computacionales (CIMEC), UNL, CONICET, Predio "Dr. Alberto Cassano", Colectora Ruta Nacional 168 s/n, 3000, Santa Fe, Argentina
[b] Grupo de Investigación en Mecánica Computacional y Estructuras (GIMCE), Facultad Regional Concepción del Uruguay (FRCU), Universidad Tecnológica Nacional (UTN), 3260, Concepción del Uruguay, Argentina

**Abstract**

In the last years, multi-objective optimization techniques became into one of the main challenges of the buildings energy efficiency area. The objective of this paper is to develop and validate a computational code for multi-objective buildings performance optimization by linking an evolutionary algorithm and a building simulation software in a powerful cluster. A sophisticated version of the multi-objective Non-dominated Sorting Genetic Algorithm-II (NSGA-II) was implemented in Python code to determine the optimal building design, which allows working with categorical and discrete variables, and the objectives were evaluated using the building energy simulation software EnergyPlus. NSGA-II was implemented to run in a high-performance cluster for the parallel computing of the fitness of each population (set of possible designs). In this work, the strengths of the proposed method were demonstrated by its application to the optimal design of a typical single-family house, located in the Argentine Littoral region. This house has some rooms conditioned only by natural ventilation, and other rooms with natural ventilation supplemented by mechanical air-conditioning (hybrid ventilation). The most influential design variables like roof types, external and internal wall types, solar orientation, solar absorptance, size, type, and windows shading of this house among others were studied in two complex cases of $10^8$ and $10^{16}$ possibilities to obtain the best trade-off (Pareto front) between heating and cooling performance. Finally, a decision-making method was applied to select one configuration of the Pareto front. Optimal simulation results for the study cases indicated that is possible to improve up to 95% the thermal comfort in naturally ventilated rooms and up to 82% energy performance in air-conditioned rooms of the building with respect to the original configuration by using a design that takes simultaneous advantage of passive strategies like thermal inertia and natural ventilation. The methodology was proved to give a robust and powerful tool to design efficient dwellings reducing the optimization time from almost 12 days to 4,4h.

*Keywords:* Multi-objective optimization, NSGA-II, Energy consumption, Thermal comfort, Hybrid ventilation, High-performance cluster application

## 1. Introduction

Today, Argentine electricity sector faces an emergency state since the operation reserve under extreme weather conditions is less than 5% of the available power, while the thermoelectric power plants (providing more than

60% of the total electric power) have low reliability, mainly because of their obsolescence, and the availability of imported gas and diesel is uncertain in the middle term [1]. Such crisis has multiple reasons [2]: the lack of state policies in the energy sector, the poor diversification of primary energy sources, the lack of criteria to reduce the energy intensity, among others.

However, even though the residential buildings are the largest energy consumers (36.3% and 46.6% of the total electricity and gas, respectively [3]), the only Argentine regulation on building energy efficiency [4] has serious gaps: 1) it is not compulsory and gives no incentive, 2) it is exclusively based on the envelope transmittance, and 3) it just addresses the labeling for heating, which is actually not the main concern in large areas of the country, including the so-called Littoral region we are particularly interested in.

Littoral is a 0.5-million km$^2$ area located in northeastern Argentina, southeastern South America, where the climate is Cfa according to the Köppen-Geiger classification [5]. More specifically, Littoral can be divided into three zones [6]: I) very hot in the north, II) hot in the center, and II) warm temperate in the south. In addition, according to the Fifth Assessment Report of the Intergovernmental Panel on Climate Change (IPCC) [7], the temperature will be 2 to 4.5°C higher by 2100 (referred to 2014) in southeastern South America. Consequently, taking as reference the work of Invidiata and Ghisi [8] on two southern Brazilian locations whose climate is close to that of Littoral, the annual energy demand is expected to increase around 200% by 2050 with respect to 2016 (while the energy demand for heating should decrease around 80% by this time).

Under these circumstances, it urges to improve the energy efficiency of buildings. To this end, a broad enough spectrum of alternative designs for a given building has to be evaluated, with each design characterized by a set of design variables like the building orientation, the type of internal and external walls and roof, the size, glazing, shading and infiltration rate of windows, the HVAC equipment, etc. Such variables are usually correlated and have a nonlinear effect on the thermal and energy response of the building. Given such complexity, recourse has to be made to building performance simulation (BPS) using general purpose software like EnergyPlus, ESP-r, and TRNSYS or dedicated codes like OBEM for office building envelopes [9].

In addition, when the number of alternatives is very large, it is necessary to automate this task and make it in an intelligent form to find a good design without the need of exploring all of these alternatives. This problem has been tackled by many authors by means of simulation-based optimization techniques. But, even if a particular design can be quickly evaluated using BPS, the usually so huge number of alternatives makes also essential to use building performance optimization (BPO), coupling BPS with a numerical optimization algorithm.

Several applications of BPO can be found in the recent literature. For instance, Islam et al. [10] coupled linear programming with AccuRate (the thermal rating tool accredited in Australia) to minimize the weighted sum of the life cycle cost and the environmental impact of residential buildings by acting on three categorical design variables (type of wall, roof and floor); Delgarm et al. [11] applied multi-objective optimization togetehr with EnergyPlus to minimize the cooling and lighting demand of a one-thermal zone building, taking as design variables the building size and orientation and the overhangs; Lu et al. [12] combined mono- and multi-objective genetic algorithms running under Matlab® with TRNSYS to optimize the renewable energy systems in low energy buildings; Yu et al. [13] used multi-objective genetic algorithms in conjunction with EnergyPlus to simultaneously maximize the thermal comfort and minimize the energy consumption in building design.

A critical aspect of BPO is the computational time to achieve optimal solutions. Some authors [14, 15] tackled this problem by using a metamodel (model of a model) of the building performance, which is previously trained on the base of a representative sample made of BPS results for different sets of design variables. The Latin Hypercube sampling (LHS) method is usually applied to obtain small yet statistically representative samples. The size of the sample is problem-dependent [16], and it can varies from 2.2$\times$ [17, 18] to 4166.6$\times$the number of design variables [19] in different BPS applications. Actually, until today, the correct size of the sample for a given building has to be determined by trial and error, which may seriously compromise the advantages of this method.

Then, the main objective of this paper is to take advantage of high performance computing as an alternative way of reducing the computational time of solving multi-objective optimization problems. To this end, we developed a Python code to use NSGA-II for multi-objective optimization, calling EnergyPlus for evaluating the fitness of a large number of individuals of a population (even the whole population itself) in parallel in a cluster.

Another contribution of this work lies in the definition of the multiple objectives, which account for the performance of a house under cooling as well as heating conditions, considering that the house has both naturally and hybrid ventilated rooms. Finally, a decision making criterion is proposed to choose the final solution from the set of optimal solutions given by NSGA-II.

The objective of this paper is to develop and validate a computational code for multi-objective buildings performance optimization by linking an evolutionary algorithm and a building simulation software in a powerful cluster.

## 2. Methodology

This section defines the architectural design of an energy efficient dwelling as a multi-objective optimization problem. In section 2.1, the different approaches for multi-objective optimization are discussed, justifying the choice of NSGA-II solver for the current work. Section 2.2 presents an automatic method for the selection of the final solution from the set of optimal solutions obtained with NSGA-II. Section 2.3 describes the current BPO implementation BPO, where NSGA-II is linked to EnergyPlus using the parallel Python library. Section 2.4 describes the building model of a typical house taken as the base case and introduces indicators of the performance of the rooms having natural ventilation either exclusively or complemented with mechanical air conditioning. These indicators serve to define the multiple objectives to be optimized, as discussed in section 2.5. Finally, section 2.6 is devoted to explain the current choice of design variables.

### *2.1. Multi-objective optimization*

The architectural design of an energetically efficient building usually faces different objectives: to improve the comfort of naturally ventilated rooms and to reduce the energy consumption in air-conditioned rooms [20], to reduce environmental impact and energy consumption while improving the indoor thermal comfort [21], to reduce the energy consumption for cooling as well as for lighting by acting on solar shading [22], to minimize the life cycle cost as well as the carbon dioxide equivalent emissions of residential buildings [23], etc.. In all these cases, the optimal design is the argument of the multi-objective optimization problem

$$\min_{\mathbf{x}} \quad [f_1(\mathbf{x}) \quad f_2(\mathbf{x}) \quad \dots \quad f_N(\mathbf{x})], \tag{1}$$

where $f_i$ denotes a specific objective and $\mathbf{x}$ is the set of design variables.

In presence of mutually conflicting objectives, the solution of problem (1) is not a unique optimal design but a set of non-dominated solutions whose locus is commonly referred to as Pareto front because of Pareto dominance concept [24]. A solution is non-dominated (or Pareto-optimal) if there is not any other feasible solution that improves one objective without deteriorating at least one another. In the case of two objectives the set of non-dominated solutions (Pareto front) is a plane curve like that depicted in Fig. 1. More precisions on the mathematical foundations of Pareto optimality can be found in the multi-objective optimization literature, e.g. [25, 26].

A first approach to solve a multi-objective optimization problem consists of defining a unique objective as the weighted sum of all the individual objectives $f_i$ (this was our choice in [20]), or as a norm of the vector of components $f_i$ (as done by Koo et al. [27], for instance). This yields a mono-objective problem, which can be solved using classic optimization algorithms. The goodness of the solution depends on the choice of the weight factors $w_i$, each choice giving a single solution of the Pareto front. If multiple solutions are desired, the problem must be solved several times with different weight combinations [28], which is more expensive than using Pareto-based optimization from the beginning. Another disadvantage of this approach is that not all the Pareto-optimal solutions can be attained when the true Pareto front is non-convex [25].

Truly multi-objective optimization solvers have been developed to overcome these problems, for instance MOPSO [29], SPA2 [30], and NSGA-II [31]. Being evolutionary algorithms, these solvers are well suited for parallel computing, do not "get stuck" in local optima, and have low sensitivity to discontinuities in the objective function, making them the preferred solvers for BPO [32, 33]. Among them, NSGA-II [31] stands out thanks to its efficient sorting of non-dominated solutions, accounting for elitism (which speeds up the convergence), and giving a set of Pareto-optimal solutions that are well distributed along the Pareto front. Because of these properties, widely appreciated in BPO [11, 13, 22, 34–37], NSGA-II was adopted for this work.

### *2.2. Decision-making process*

Once the set of Pareto-optimal solutions (or Pareto front) $\mathbf{x}_1^{\text{opt}}, \mathbf{x}_2^{\text{opt}}, \dots, \mathbf{x}_P^{\text{opt}}$ (with $P$ denoting the population size) was obtained (using NSGA-II, for instance), a decision must be made to determine the final optimal solution $\mathbf{x}^{\text{opt}}$ among them. Such a decision depends on the relative importance of the objective functions, whose a priori assessment relies on the user's expertise. Here, we propose to use an automated decision-making strategy based on the distance of the Pareto-optimal solutions to the "ideal point", defined as the set of the best solutions to each independent problem [38], i.e.

$$\mathrm{P}_{\mathrm{ideal}} = [\min(f_1) \quad \min(f_2) \quad \dots \quad \min(f_N)]. \tag{2}$$

Normally, this point is not attainable in a multi-objective optimization problem because these objectives cannot be minimized simultaneously due to their conflicting nature [38].

The distance of a Pareto-optimal $\mathbf{x}_k^{\mathrm{opt}}$ to the ideal point is determined as

$$\mathrm{d}(\mathbf{x}_k^{\mathrm{opt}}) = \sqrt{\left[f_1(\mathbf{x}_k^{\mathrm{opt}}) - \min(f_1)\right]^2 + \left[f_2(\mathbf{x}_k^{\mathrm{opt}}) - \min(f_2)\right]^2 + \cdots + \left[f_N(\mathbf{x}_k^{\mathrm{opt}}) - \min(f_N)\right]^2} \tag{3}$$

Then, the final optimal solution $\mathbf{x}^{\mathrm{opt}}$ is defined as that Pareto-optimal with the shortest distance to the ideal point. Fig. 1 schematizes the Pareto front, the ideal point and the final optimal solution for the problem of minimizing two conflicting objectives.

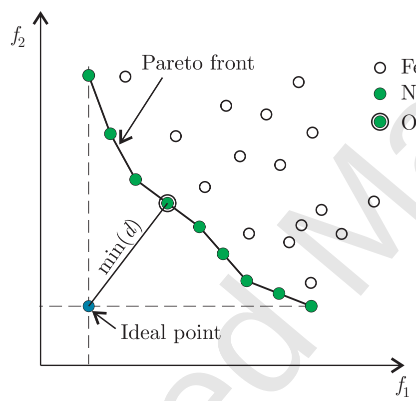


Figure 1. Schema of the Pareto front, the ideal point, and the final optimal solution for the minimization of two contradictory objectives $f_1$ and $f_2$.

### *2.3. Current multi-objective BPO implementation*

The multi-objective BPO methodology applied in this work consists of using NSGA-II [31] as optimization solver combined with EnergyPlus ($E^+$) [39] for fitness evaluation. We took as platform the Distributed Evolutionary Algorithms in Python (DEAP) [40], which includes the NSGA-II solver as it was revisited by Fortin et al. [41]. Furthermore, in order to improve the performance of this solver in presence of integer design variables, we implemented Laplace crossover and power mutation techniques [42] to replace the binary crossover and the polynomial mutation used in the NSGA-II proposed by Fortin et al. [41].

The core of the NSGA-II is a genetic algorithm [43], where a population of individuals is randomly seeded, then undergoes mutation (random changes) and crossover (interpolation between individuals). A selection process is used to find high-performing individuals to form the next generation. The process is then repeated for a given number of generations. In particular, for NSGA-II, the individuals are selected by non-domination rank taking as many complete ranks as will fit in the new population. Any remaining spaces are then filled according to crowding distance. This selection process drives the population towards the optimum Pareto front while maintaining diversity along the front [31].

Briefly, the steps of NSGA-II are summarized in the following pseudo-code:

```
pop = random(popsize)
Fitness(pop)
pop = Selection(pop)
From 1 to #generations do
       offspring = Non-dominated-selection(pop)
       offspring = Crossover(offspring)
       offspring = Mutation(offspring)
       Fitness(offspring)
       pop = selection (offspring)
End
```

At each fitness step, the objectives $f_i(\mathbf{x}_j)$ are calculated for each individual $\mathbf{x}_j$ $(j = 1, 2, \ldots, P)$ in the population. To this end, we wrote a Python routine that reads $\mathbf{x}_j$ from the mutation offspring (that is, from DEAP), converts the entries of $\mathbf{x}_j$ in $E^+$ inputs, writes the corresponding $E^+$ input file (.idf), calls $E^+$ to run this file and reads the $E^+$ output file to finally determine $f_i(\mathbf{x}_j)$. This DEAP/$E^+$ interface makes use of the Parallel Python library [44], enabling a whole population to be evaluated at once taking advantage of parallel computing. Here, we used the Pirayu cluster [45] installed in our laboratory.

Fig. 2 shows the diagram of the computational implementation of the proposed multi-objective BPO methodology.

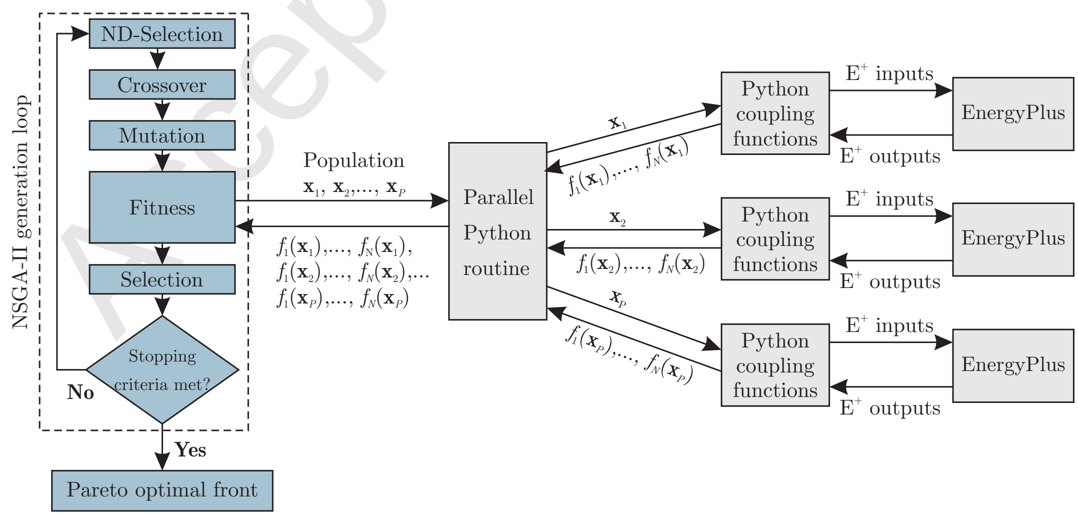


Figure 2. Diagram of the computational implementation of the current multi-objective BPO methodology.

### 2.4. Case study

Without a reference house for energy efficiency in Argentine building regulations, we adopted as typical house the so-called Roble2D house funded by PROCREAR [46] (a massive credit program subsidized by the Argentine national government). The Roble2D house is a 83 m$^2$ two-story, detached house with the kitchen, the living room and a bathroom on the ground floor, and two bedrooms, a corridor, and a bathroom on the first floor, as shown in Fig. 3. It is assumed to be located at Paraná, a city in the center of Littoral with latitude 31.78S, longitude 60.48W and altitude 78 m.a.s.l.. We have recently generated the typical meteorological year (TMY) at 15 locations in Littoral [47], including Paraná, for which files in EPW format are available online [48, 49].

This is the same case study that was widely detailed in our previous work [20]. For the sake of completeness, the main features of this house and its BPS model will be recalled here. The original configuration of the Roble2D house, say Case 0, is summarized in Table 1.


Figure 3. Roble2D single-family house from the Argentine credit program PROCREAR.

The E$^+$ version 8.4.0 [50] to evaluate the thermal and energy performance of this house and its alternative designs was used. In all cases, the house was divided into eight thermal zones, corresponding to the kitchen, the living room, the two bathrooms, the two bedrooms, the corridor and the staircase of the Roble2D house, see Fig. 3. Each zone was assimilated to a *FullExterior* E$^+$ object [51], where the effect of shadows on the external surfaces is accounted for.

The Roble2D house is planned to be occupied by four people. In particular, we assumed each bedroom and the living room to accommodate two and four people, respectively, according to the schedules depicted in Fig. 4. Each one of these rooms had its respective internal heat load coming from the occupants, the lighting and the equipment, following ASHRAE [52].

Table 1. Original configuration (Case 0) of the *Roble2D* single-family house.

| **Element** | **Characteristics** |
|---|---|
| Building azimuth | 0 (surface 1 facing North) |
| Type of external walls | Hollow brickwork layer with mortar finish |
| External solar absorptance of external walls | 0.7 |
| Type of windows | Simple clear 3 mm-thick glass |
| Shading fraction in windows | 25% |
| Infiltration rate in windows and doors | 0.02 kg/s/m |
| Window area fraction for natural ventilation | 30% |
| Type of roof | Ceramic tile, air gap and concrete liner |
| Type of internal walls | Hollow brickwork layer with mortar finish |
| Type of the first floor | Concrete with ceramic floor |

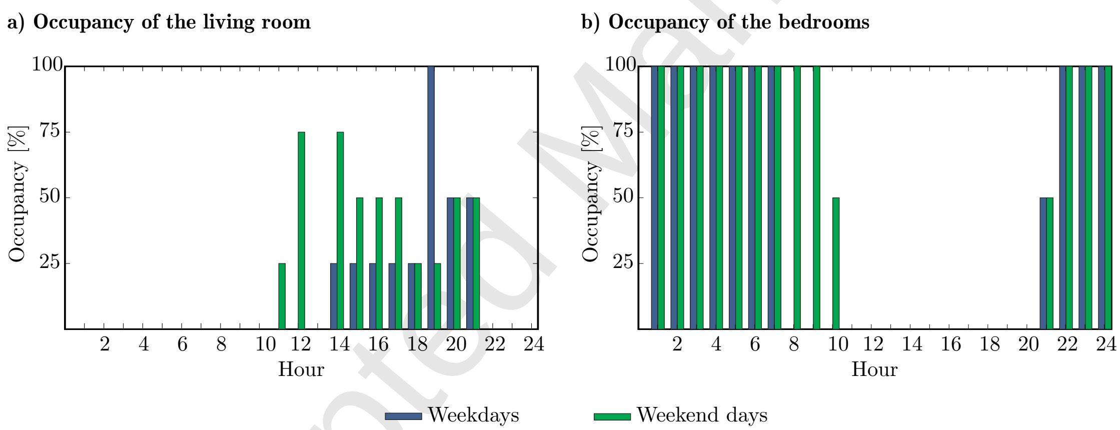


Figure 4. Schedules of occupancy for the living room and the bedrooms.

*2.4.1. Measurement of performance for naturally-ventilated rooms*

In a naturally-ventilated room, the thermal discomfort is measured using the cooling and heating degree-hours, defined as

$$D_{\mathrm{cool}} = \sum_h \langle T_{\mathrm{op}}(h) - T_{\mathrm{upper}}(h) \rangle \,, \tag{4}$$

$$D_{\mathrm{heat}} = \sum_h \langle T_{\mathrm{lower}}(h) - T_{\mathrm{op}}(h) \rangle \,, \tag{5}$$

respectively, where $\langle x \rangle$ is the ramp function ($\langle x \rangle = 0$ if $x < 0$ and $\langle x \rangle = x$ if $x \geq 0$), $T_{\mathrm{op}}(h)$ is the operative temperature in the room at the hour $h$ (obtained as an output of E$^+$), $T_{\mathrm{lower}}$ and $T_{\mathrm{upper}}$ are the lower and upper admissible temperature; the range of the preceding sums is a whole year, excluding the hours when the room is not occupied.

The admissible temperatures $T_{\text{lower}}$ and $T_{\text{upper}}$ were defined as the lower and upper 80%-acceptability limits [53]:

$$T_{\text{lower}} = 0.31\, T_{\text{pma(out)}} + 14.3°\text{C}, \tag{6}$$

$$T_{\text{upper}} = 0.31\, T_{\text{pma(out)}} + 21.3°\text{C}, \tag{7}$$

where $T_{\text{pma(out)}}$ is the prevailing mean outdoor temperature, which is assumed to be the monthly mean of the local dry-bulb temperature, as shown in Fig. 5.

In the current house, all the rooms except the bathrooms were assumed to be naturally ventilated, being modeled as *AirflowNetwork* $\text{E}^+$ objects where windows and doors are temperature-controlled in order to allow airflow when the indoor temperature was higher than the outdoor and whenever the outdoor temperature was higher than 20°C.

Here, only the living room was considered for computing $D_{\text{heat}}$ and $D_{\text{cool}}$. It is actually the busiest naturally-ventilated room, occupied according to the schedule in Fig. 4a.

### *2.4.2. Measurement of performance for hybrid rooms*

In those rooms where the thermal comfort is artificially enforced if necessary, the thermal performance is rather measured by means of the annual energy consumption of the air conditioners for heating and cooling, say $E_{\text{heat}}$ and $E_{\text{cool}}$ respectively.

This is the case of the bedrooms of the currently studied house, where the air-conditioner was turned on (and the airflow was blocked) whenever natural ventilation was not enough for ensuring the thermal comfort. This combined use of active and passive cooling and heating strategies is accounted for using the $\text{E}^+$ *HybridVentilation Manager*. The air-conditioners in the bedrooms were modelled as packaged terminal heat pumps (PTHP). They were allowed to work for heating when the room temperature was less than or equal to 18°C, and for cooling when the room temperature was greater than or equal to 26°C, whenever the bedrooms were occupied at the given hour $h$ (see the schedule of occupancy of the bedrooms in Fig. 4b).

### *2.5. Definition of the objective functions*

As was mentioned before, the degree-hours in the naturally-ventilated living room and the energy consumption in hybrid bedrooms are assumed as indicators of the energy performance of dwellings. Other aspects of indoor environmental quality, such as visual comfort, acoustic comfort and indoor air quality, have not been included in this work.

Then, we define the optimal design of a house as the solution of the multi-objective optimization problem

$$\min_{\mathbf{x}}\ [f_{\text{heat}}(\mathbf{x}) \quad f_{\text{cool}}(\mathbf{x})\,] \tag{8}$$

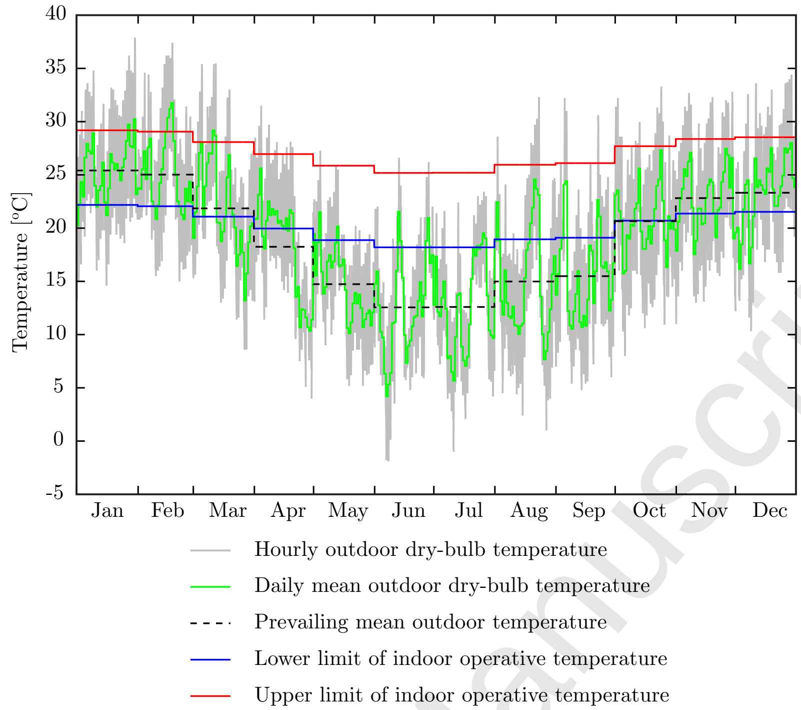


Figure 5. Mean hourly and daily dry-bulb temperature, prevailing mean outdoor air temperature, and 80% acceptability limits for the city of Paraná.

with the objective functions defines as:

$$f_{\text{heat}}(\mathbf{x}) = w_D \frac{D_{\text{heat}}(\mathbf{x})}{D_{\text{heat}}(\mathbf{x}_0)} + w_E \frac{E_{\text{heat}}(\mathbf{x})}{E_{\text{heat}}(\mathbf{x}_0)}, \tag{9}$$

$$f_{\text{cool}}(\mathbf{x}) = w_D \frac{D_{\text{cool}}(\mathbf{x})}{D_{\text{cool}}(\mathbf{x}_0)} + w_E \frac{E_{\text{cool}}(\mathbf{x})}{E_{\text{cool}}(\mathbf{x}_0)}, \tag{10}$$

where $w_D$ and $w_E = 1 - w_D$ are weighting factors, and $\mathbf{x}_0$ is the set of design variables for Case 0, see Table 1.

Note that each objective is at its turn a weighted sum of two sub-objectives. Each subobjective (either $D_{\text{heat}}$, $E_{\text{heat}}$, $D_{\text{cool}}$ or $E_{\text{cool}}$) is an $\text{E}^+$ output. In order to combine the degree-hours and the energy consumption, these sub-objectives were normalized with respect to a baseline case (here, Case 0), as frequently done in BPO [10, 20, 28]. Regarding the weighting factors, there is no rule to select them. Here, taking into account that the periods of occupancy of the living room (involved in $D_{\text{heat}}$ and $D_{\text{cool}}$) and the bedrooms (involved in $E_{\text{heat}}$ and $E_{\text{cool}}$) were similar in extension, we set $w_D = w_E = 0.5$, a choice that was validated by the results to be discussed in section 3.

*2.6. Specification of the design variables*

In a previous work [20], the Morris screening method [54] was used to determine the sensitivity of the subobjectives $D_{\text{heat}}$, $E_{\text{heat}}$, $D_{\text{cool}}$, and $E_{\text{cool}}$ with respect to a large set of design variables. From this analysis, we determined a set of 12 design variables $x_i$ to be the most relevant ones. Among them, some variables, like the building azimuth and, the windows shading size, are continuous within a certain interval; these are the variables

$x_1, x_2, \ldots, x_7$ in Table 2 . Other variables, like roof type, external walls type, window type, etc., are categorical, being listed in Table 3. The material properties associated with these categorical variables are those defined by the Argentine standard IRAM 11603 for thermal conditioning of buildings [6], shown in Table 4.

Table 2. Continuous design variables and their discretization.

| Variable | Description | Minimum | Maximum | Step | #Levels |
|---|---|---|---|---|---|
| $x_1$ | Building azimuth | 0° | 315° | 45° | 8 |
| $x_2$ | Window shading size | 25% | 100% | 25% | 4 |
| $x_3$ | Solar absorptance of external walls | 0.3 | 0.9 | 0.2 | 4 |
| $x_4$ | Windows infiltration rate | $10^{-5}$ kg/s/m | $2 \times 10^{-2}$ kg/s/m | $6.67 \times 10^{-3}$ kg/s/m | 4 |
| $x_5$ | Doors infiltration rate | $10^{-5}$ kg/s/m | $2 \times 10^{-2}$ kg/s/m | $6.67 \times 10^{-3}$ kg/s/m | 4 |
| $x_6$ | Window area fraction for natural ventilation | 10% | 50% | 10% | 5 |
| $x_7$ | Window width [level]* | 1 | 4 | 1 | 4 |

* Windows width becomes a categorical variable after discretization.

While the categorical variables are intrinsically discrete, we decided to discretize the continuous variables, that is, only certain discrete values or "levels" of them were allowed, mainly to account for constraints of the house building process. For instance, the azimuth $x_1$ was allowed to have eight levels: from 0° to 315° every 45°.

A particular way of discretization was applied to the window width. The corresponding variable $x_7$ had four levels, each one denoting a different width depending on the façade containing the window: 0.70 m, 1.35 m, 2.00 m, 2.70 m for surface 1; 0.70 m, 1.60 m, 2.50 m, 3.40 m for surface 3; 0.70 m, 1.40 m, 2.15 m, 2.90 m for surface 4.

Note that the azimuth $x_1$ was more finely discretized than the other variables, as a result of the sensitivity analysis [20], where we found it to have a strong nonlinear effect on the outputs, and to be highly correlated with other variables.

Let Case A denote the optimization problem (8) with these 12 recently described design variables, listed in Tables 2 and 3.

Now, let us define a more sophisticated optimization problem, say Case B, having the same objectives but 22 design variables. The new variables are the type of wall, external solar absorptance, window width and window shading size, which are now associated to each external surface. For instance, the unique variable $x_8$ defining the type of all the external walls in Case A was replaced by four variables, each one defining the type of wall at one of the external surfaces of the house. Furthermore, each one of the new variables replacing the variable $x_i$ in Case A has the same levels as $x_i$.

## 3. Results

This section summarizes the results of solving the optimization problem (8) for Cases A and B, that is, with 12 or 22 variables respectively. In both cases, the optimization problem was solved using NSGA-II, setup as

Table 3. Categorical design variables.

| Variable | Description | Level |
|---|---|---|
| $x_8$ | External walls | 1: Wood with air gap<br>2: Hollow brickwork layer with mortar finish<br>3: Double hollow brickwork layers with insulation and mortar finish<br>4: Wood with insulation and plaster finish<br>5: Concrete block with cement-plaster finish<br>6: Double concrete block with insulation and cement-plaster finish<br>7: Concrete |
| $x_9$ | Roof type | 1: Concrete with plaster ceiling<br>2: Concrete and hollow ceramic block with plaster ceiling<br>3: Ceramic tile, air gap and wood liner<br>4: Ceramic tile, air gap and concrete liner<br>5: Ceramic tile, air gap, insulation and concrete liner<br>6: Ceramic tile, air gap, insulation and wood liner |
| $x_{10}$ | Window type | 1: Single clear 3 mm thick glass<br>2: Single clear 6 mm thick glass<br>3: Double clear 3 mm thick glass with air gap<br>4: Double clear 3 mm thick glass with air gap |
| $x_{11}$ | Internal walls | 1: Wood with air gap<br>2: Hollow brickwork layer with mortar finish<br>3: Wood with insulation and plaster finish<br>4: Concrete block with cement-plaster finish<br>5: Concrete |
| $x_{12}$ | Floor type of the first floor | 1: Concrete with ceramic floor<br>2: Concrete with wood floor<br>3: Insulation, concrete and ceramic floor |



shown in Table 5.

### *3.1. Optimization of Case A*

Considering Case A, Fig. 6 shows the trade-off between the optimal solutions for $f_{\text{heat}}$ and $f_{\text{cool}}$, where it is apparent their conflicting nature. Note that $f_{\text{cool}} \approx 2.9$ is very large for the optimal heating solution $f_{\text{heat}} \approx 0$, while $f_{\text{heat}} \approx 0.5$ is not as bad for the optimal cooling solution $f_{\text{cool}} \approx 0.1$. So, it is considerably easier to improve the design for heating than for cooling, which is not surprising because of the hot weather at the chosen location.

Table 4. Thermal transmitance $U$, thermal capacity $C_t$, and thermal delay $\theta$ for the different cases of external walls, roof, internal walls, and floor type of the fist floor.

| **Design variable** | **Level** | $U$ [W/m$^2$/K] | $C_t$ [kJ/m$^2$/K] | $\theta$ [hours] |
|---|---|---|---|---|
| External walls | 1 | 1.99 | 64.32 | 2.75 |
| | 2 | 2.09 | 136.06 | 3.38 |
| | 3 | 0.93 | 189.34 | 7.38 |
| | 4 | 0.88 | 59.21 | 3.65 |
| | 5 | 2.78 | 124.95 | 3.06 |
| | 6 | 0.87 | 233.30 | 9.71 |
| | 7 | 4.32 | 240.00 | 2.40 |
| Roof type | 1 | 3.68 | 195.36 | 2.15 |
| | 2 | 2.59 | 90.79 | 1.53 |
| | 3 | 2.03 | 38.91 | 1.31 |
| | 4 | 2.06 | 216.84 | 4.78 |
| | 5 | 0.83 | 217.85 | 9.08 |
| | 6 | 0.83 | 39.92 | 2.55 |
| Internal walls | 1 | 1.99 | 64.32 | 2.75 |
| | 2 | 2.09 | 136.06 | 3.38 |
| | 3 | 0.88 | 59.21 | 3.65 |
| | 4 | 2.78 | 124.95 | 3.06 |
| | 5 | 4.32 | 240.00 | 2.40 |
| Floor type of the first floor | 1 | 4.71 | 256.56 | 2.68 |
| | 2 | 2.59 | 213.44 | 4.36 |
| | 3 | 0.61 | 258.59 | 12.94 |

The optimal heating and cooling solution, say $\mathbf{x}_{\mathrm{A}}^{\mathrm{opt}}$, defined to be the closest to the utopia point, is given in Table 6.

Taking as reference the Case 0 defined by the set of design variables $\mathbf{x}_0$ (see Table 1), for which $f_{\mathrm{heat}}(\mathbf{x}_0) = f_{\mathrm{cool}}(\mathbf{x}_0) = 1$, it is clear that the thermal and energy performance of the house was hugely improved via optimization: $f_{\mathrm{heat}}(\mathbf{x}_{\mathrm{A}}^{\mathrm{opt}}) = 0.048$, $f_{\mathrm{cool}}(\mathbf{x}_{\mathrm{A}}^{\mathrm{opt}}) = 0.147$.

Now, let us disaggregate the results: on the one hand, $E_{\mathrm{heat}}$ vs. $E_{\mathrm{cool}}$ (Fig. 7a) and, on the other hand, $D_{\mathrm{heat}}$ vs. $D_{\mathrm{cool}}$ (Fig. 7b). In both cases, results are very close to those obtained for $f_{\mathrm{heat}}$ vs. $f_{\mathrm{cool}}$ in terms of trade-off between conflicting objectives. Actually, the optimal heating and cooling solution is identical for the three cases.

Table 5. Settings of NSGA-II for the current problems.

| | **Case A** | **Case B** |
|---|---|---|
| Population size | 64 | 64 |
| Number of generations | 100 | 150 |
| Selection | Tournament | |
| Non-dominated selection | TournamentDCD | |
| Crossover method | Laplace crossover | |
| Crossover probability | 95% | 95% |
| Mutation method | Power mutation | |
| Mutation probability | 0.5% | 0.5% |

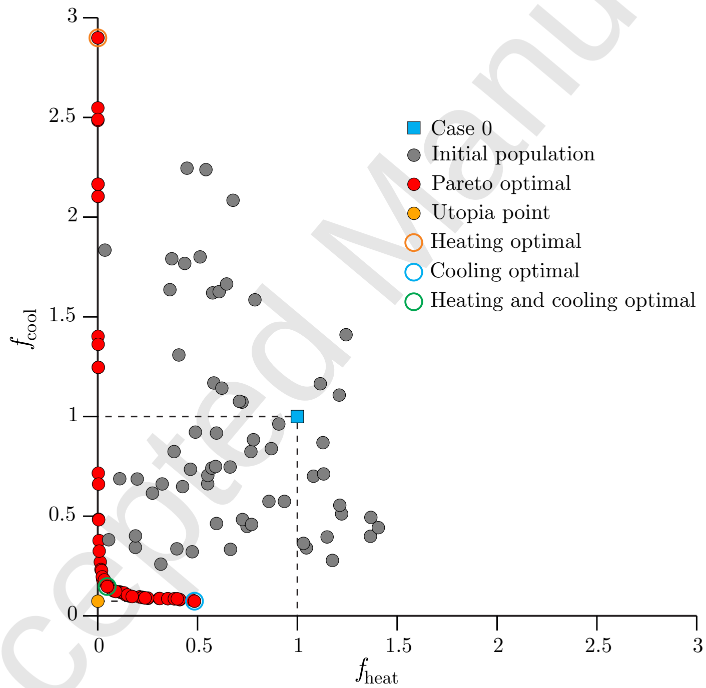


Figure 6. Case A: Trade-off between the contradictory global objectives $f_{\text{heat}}$ and $f_{\text{cool}}$ (heating and cooling performance, respectively).



But this denormalized analysis serves to highlight the improvement of the thermal and energy performance of the given house by comparing the optimal design $\mathbf{x}_{\text{A}}^{\text{opt}}$ with the original one $x_0$:

$$D_{\text{heat}}(\mathbf{x}_{\text{A}}^{\text{opt}}) = 0.083 D_{\text{heat}}(\mathbf{x}_0), \qquad D_{\text{cool}}(\mathbf{x}_{\text{A}}^{\text{opt}}) = 0.020 D_{\text{cool}}(\mathbf{x}_0),$$

$$E_{\text{heat}}(\mathbf{x}_{\text{A}}^{\text{opt}}) = 0.020 E_{\text{heat}}(\mathbf{x}_0), \qquad E_{\text{cool}}(\mathbf{x}_{\text{A}}^{\text{opt}}) = 0.202 E_{\text{cool}}(\mathbf{x}_0).$$

In addition, these results confirm that the minimization of $f_{\text{heat}}$ was closely accompanied by the minimization of the subobjectives $D_{\text{heat}}$ and $E_{\text{heat}}$, validating our decision of defining $f_{\text{heat}}$ as the weighted sum of $D_{\text{heat}}$ and

Table 6. Case A: Design variables for the optimal heating and cooling solution.

| **Design variable** | **Optimum** |
| --- | --- |
| Building azimuth | 270°C (surface 4 facing North) |
| Window shading size | 100% |
| Solar absorptance of external walls | 0.5 |
| Windows infiltration rate | $10^{-5}$ kg/s/m |
| Doors infiltration rate | 0.02 kg/s/m |
| Ventilation area fraction | 50% |
| Window width | Level 3 |
| External walls | Level 6 |
| Roof type | Level 5 |
| Window type | Level 4 |
| Internal walls | Level 5 |
| Floor type of the first floor | Level 1 |

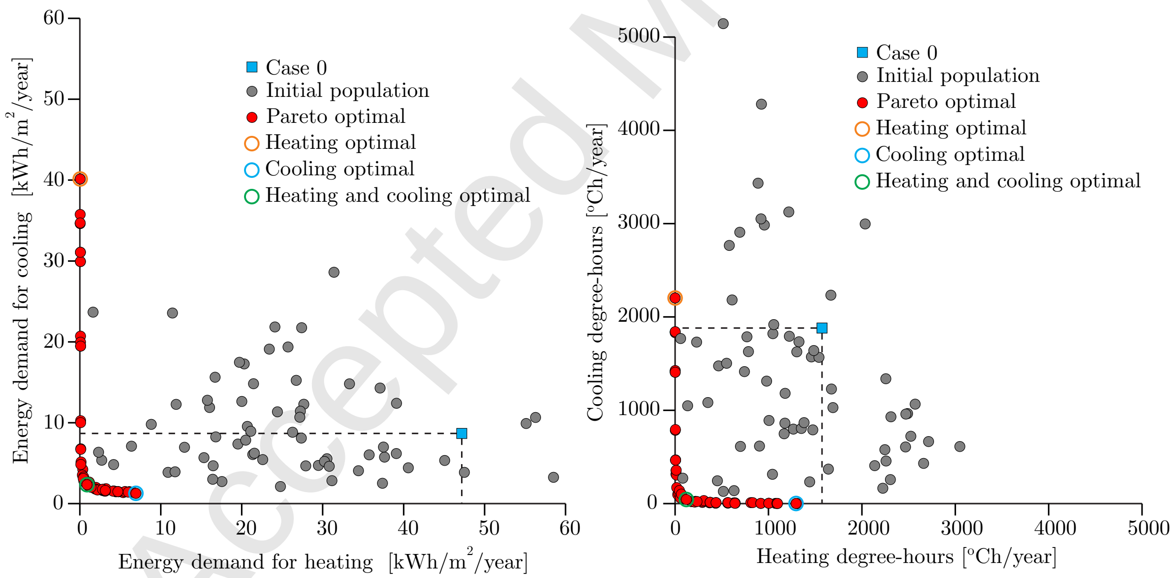


Figure 7. Case A: Trade-off between energy consumed by air-conditioners to heat and to cool the bedrooms (on the left) and between the heating and cooling degree-hours in the living room (on the right).

$E_{\text{heat}}$ as well as the current choice of the weighting factors. The same is true for $f_{\text{cool}}$ as the weighted sum of $D_{\text{cool}}$ and $E_{\text{cool}}$.

A final aspect to emphasize is the convexity of the Pareto front for the current choice of objective functions.

### 3.2. Optimization of Case B

Regarding to Case B, Fig. 8 shows the results of minimizing $f_{\text{heat}}$ and $f_{\text{cool}}$, and Fig. 9 shows results for $E_{\text{heat}}$ vs. $E_{\text{cool}}$ and $D_{\text{heat}}$ vs. $D_{\text{cool}}$ separately. In all the cases, the trade-off between conflicting objectives is similar to that observed for Case A.

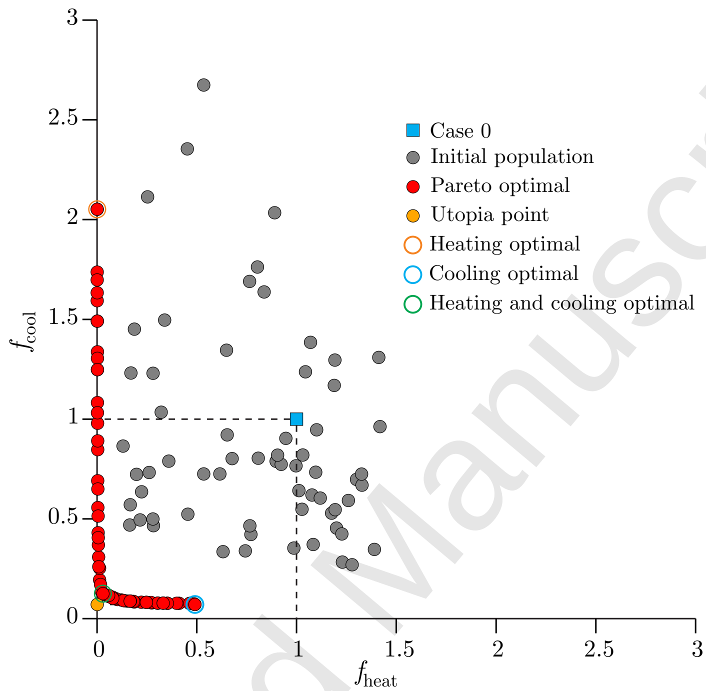


Figure 8. Case B: Trade-off between the contradictory global objectives $f_{\text{heat}}$ and $f_{\text{cool}}$ (heating and cooling performance, respectively).

The optimal heating and cooling design $\mathbf{x}_{\text{B}}^{\text{opt}}$ for Case B is given in Table 7. The thermal and energy performance of the so-designed alternative of the Roble2D house is not only much better than that of the original one (Case 0) but is also considerably better than that of Case A optimal, as shown below:

$$
\begin{aligned}
&f_{\text{heat}}(\mathbf{x}_{\text{B}}^{\text{opt}}) = 0.029 f_{\text{heat}}(\mathbf{x}_0) = 0.615 f_{\text{heat}}(\mathbf{x}_{\text{A}}^{\text{opt}}), && f_{\text{cool}}(\mathbf{x}_{\text{B}}^{\text{opt}}) = 0.125 f_{\text{cool}}(\mathbf{x}_0) = 0.851 f_{\text{cool}}(\mathbf{x}_{\text{A}}^{\text{opt}}),\\
&D_{\text{heat}}(\mathbf{x}_{\text{B}}^{\text{opt}}) = 0.055 D_{\text{heat}}(\mathbf{x}_0) = 0.666 D_{\text{heat}}(\mathbf{x}_{\text{A}}^{\text{opt}}), && D_{\text{cool}}(\mathbf{x}_{\text{B}}^{\text{opt}}) = 0.004 D_{\text{cool}}(\mathbf{x}_0) = 0.176 D_{\text{cool}}(\mathbf{x}_{\text{A}}^{\text{opt}}),\\
&E_{\text{heat}}(\mathbf{x}_{\text{B}}^{\text{opt}}) = 0.008 E_{\text{heat}}(\mathbf{x}_0) = 0.403 E_{\text{heat}}(\mathbf{x}_{\text{A}}^{\text{opt}}), && E_{\text{cool}}(\mathbf{x}_{\text{B}}^{\text{opt}}) = 0.184 E_{\text{cool}}(\mathbf{x}_0) = 0.910 E_{\text{cool}}(\mathbf{x}_{\text{A}}^{\text{opt}}).
\end{aligned}
$$

The most prominent improvement associated to $\mathbf{x}_{\text{B}}^{\text{opt}}$ concerns the cooling degree-hours in the naturally-ventilated living room: only 7.8°Ch/year.

Table 8 gives a quantitative idea of all the improvements in the thermal and energy performance of the Roble2D house enabled by optimization.

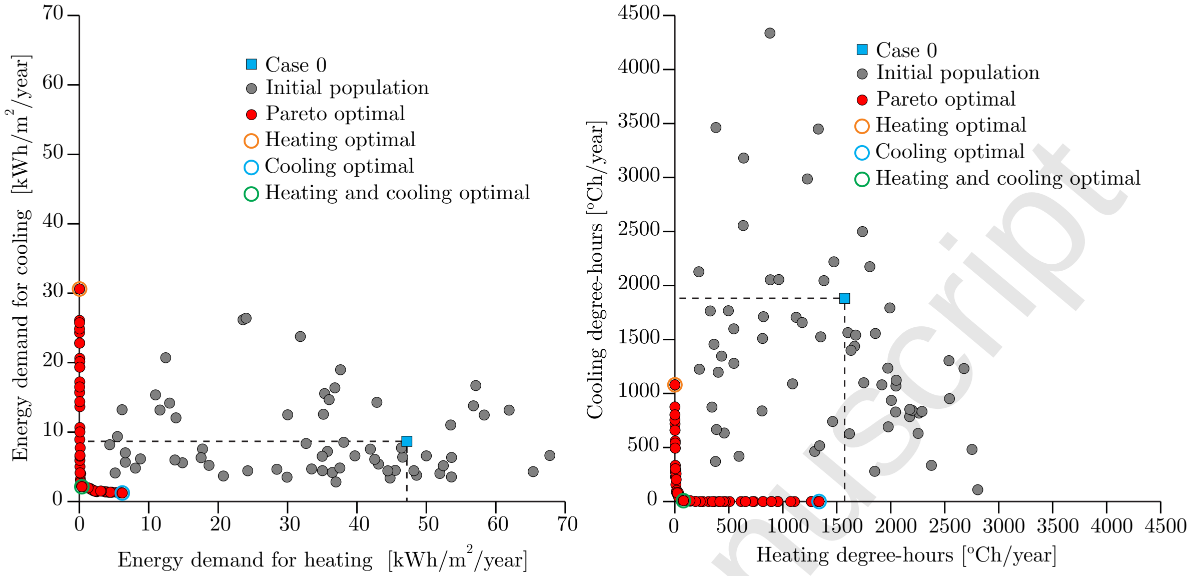


Figure 9. Case B: Trade-off between energy consumed by air-conditioners to heat and to cool the bedrooms (on the left) and between the heating and cooling degree-hours in the living room (on the right).

*3.3. Discussion on optimal solutions*

In this section, let us go into detail about the performance of the optimally designed house, either for Case A or B, compared to its initial performance (corresponding to Case 0, see Table 1).

Considering the bedrooms and the energy demand for their air-conditioning, Fig. 10, the original design was highly inefficient, especially in the heating case. Using the optimal designs, either A or B, there is energy demand for heating only from May to July (austral winter), and it is less than 2% of the energy needed by Case 0 for heating along the year. For cooling, the energy demand appears during the spring and summer (October to March) for the optimal designs, while it is also needed during the first half of the autumn for Case 0. Annually, the optimal cooling demand is just a fourth of that of the original design.

Regarding the naturally-ventilated living room, the operative temperature $T_{\mathrm{opt}}$ all along the year for the reference as well as for the optimal designs is shown in Fig. 11. Evidently, $T_{\mathrm{opt}}$ for Case 0 is mostly out of the 80%-acceptability comfort range, while it is mostly acceptable for the optimal cases. Differences between the optimal Case A and B are mainly observed in the extreme periods (mid-summer and mid-winter), being usually Case B the better one. In any case, note that there are periods when $T_{\mathrm{opt}}$ is out of the comfort range but the living room is not occupied, so they do not affect the computation of $D_{\mathrm{heat}}$ and $D_{\mathrm{cool}}$.

It is also interesting to evaluate the performance of the optimal designs compared to the reference one in those days of extreme hot and cold weather, namely January 9$^{\mathrm{th}}$ (mid-summer) and July 10$^{\mathrm{th}}$ (mid-winter). The operative temperature along these days is shown in Fig. 12. Note that Case 0 is always out of comfort during the occupied hours of the living room in these extreme days. During the extremely hot day, the living room is

Table 7. Case B: Design variables for the optimal heating and cooling solution.

| Design variable | Surface | Optimum |
|---|---|---|
| Building azimuth | | 270° (surface 4 facing North) |
| Window shading size | 1 | 75% |
| | 3 | 100% |
| | 4 | 50% |
| Solar absorptance of external walls | 1 | 0.3 |
| | 2 | 0.3 |
| | 3 | 0.7 |
| | 4 | 0.9 |
| Windows infiltration rate | | $10^{-5}$ kg/s/m |
| Doors infiltration rate | | 0.02 kg/s/m |
| Ventilation area fraction | | 50% |
| Windows width | 1 | Level 1 |
| | 3 | Level 1 |
| | 4 | Level 4 |
| External walls | 1 | Level 6 |
| | 2 | Level 6 |
| | 3 | Level 6 |
| | 4 | Level 6 |
| Roof type | | Level 5 |
| Window type | | Level 4 |
| Internal walls | | Level 5 |
| Floor type of the first floor | | Level 3 |

Table 8. Thermal and energy performance for Case 0 (reference) and the optimal solutions of Cases A and B.

| Objective | Case 0 | Case A | Case B |
|---|---|---|---|
| $f_{\text{heat}}$ | 1 | 0.05 | 0.03 |
| $f_{\text{cool}}$ | 1 | 0.15 | 0.13 |
| Heating degree-hours [°Ch/year ] | 1454.41 | 120.47 | 80.25 |
| Cooling degree-hours [°Ch/year ] | 2235.78 | 44.51 | 7.84 |
| Heating energy demand [kWh/m$^2$/year ] | 44.39 | 0.88 | 0.35 |
| Cooling energy demand [kWh/m$^2$/year ] | 11.57 | 2.34 | 2.13 |

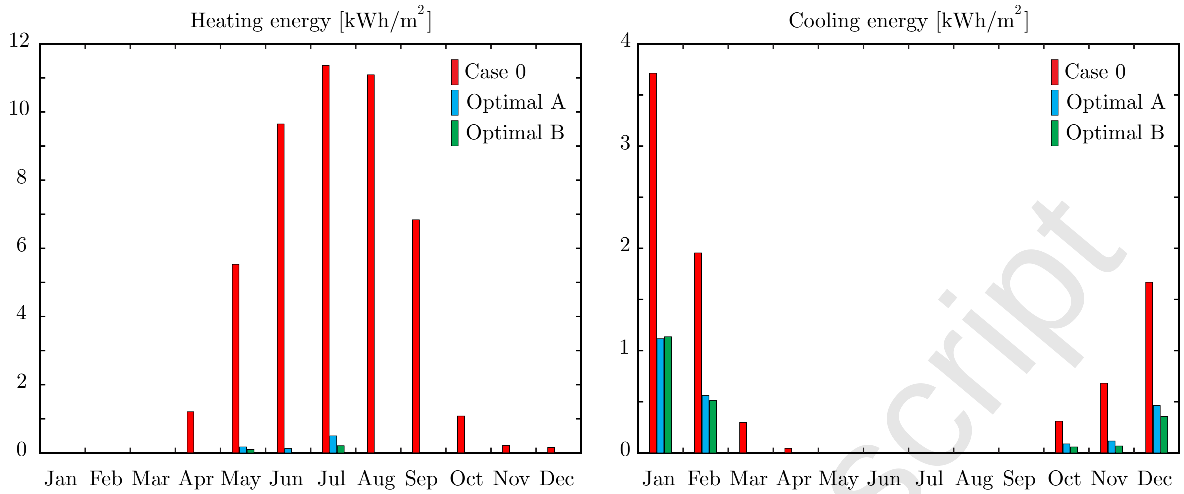


Figure 10. Monthly heating and cooling energy consumption in bedrooms for the analyzed cases.

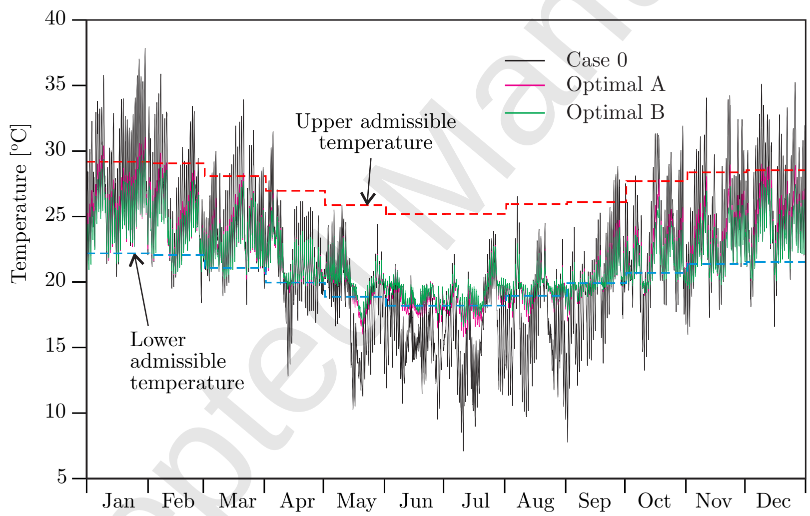


Figure 11. Hourly operative temperature at the living room for the original and the optimal designs.

90% of the occupied hours outside the comfort range for Case A, while this percentage falls to 30 for Case B (with no more than 0.2°C in excess). During the extremely cold day, the living room is 70% of the occupied hours outside the comfort range for Case A, while this percentage falls to 10 for Case B (with no more than 0.1°C in defect).

So, it can be concluded that Case B gives not only an optimal solution considering a whole year, but it also performs well during the coldest and hottest days. We found this is the main reason to prefer Case B optimal to of Case A one as the optimal design of the Roble2D house.

Let us evaluate the design corresponding to the heating and cooling optima A and B given by Tables 6 and 7 respectively, in order to find out the best architectural practices for such a typical house in the Littoral region.

The optimal azimuth was 270° for both cases, corresponding to surface 4 (actually, the largest windowed

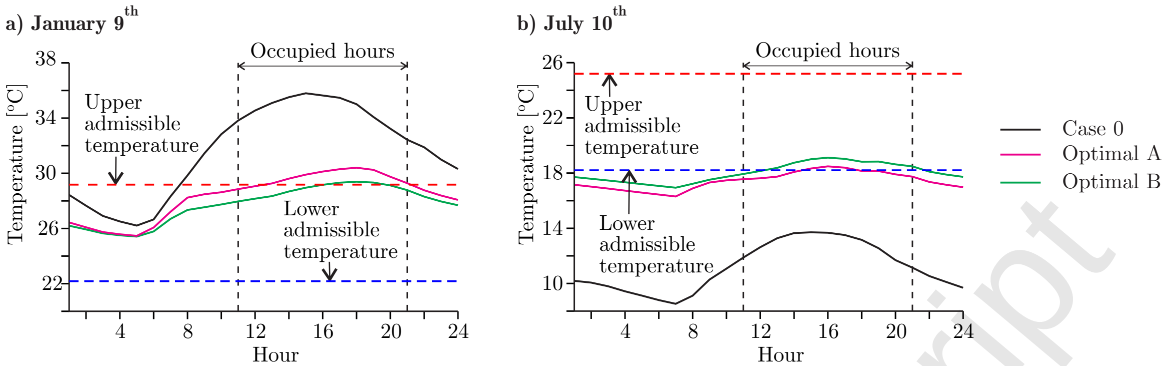


Figure 12. Hourly operative temperature at the living room for the original and the optimal designs during extreme days: a) January $9^{\text{th}}$ (mid-summer); b) July $10^{\text{th}}$ (mid-winter).

one) facing North.

The optimal windows width was Level 3 for Case A (that is, for all windows). Note that Level 3 amounts for different width magnitudes depending on the surface containing the window, as explained in Section 2.6, but it always denotes the second largest one among the four assumed levels of window width. For Case B, the optimal window width was Level 1 (the narrowest) for surfaces 1 and 3 facing West and East respectively, and Level 4 (the widest) for the North-facing surface 4.

The optimal shading for Case A is 100% for all the windows. For Case B, the windows facing East and West were well shaded, while those facing North were 50% shaded.

The optimal window area fraction for natural ventilation was 50% in both cases, which was the maximal prescribed level.

The optimal external thermal absorptance was 0.5 for Case A for all the surfaces, while it was 0.9 (upper bound) for the North-facing surface, 0.75 for the South-facing surface, and 0.3 (lower bound) for the East- and West-facing surfaces.

The optimal external wall was Level 6 for both cases. Compared to the other admitted choices, Level 6 has low thermal transmittance, high thermal capacity and high delay, as shown in Table 4.

The floor of the first floor was Level 1, having the highest thermal transmittance, a high thermal capacity and lowest thermal delay in Case A. In Case B, Level 3 was chosen, having the lowest transmittance and the highest thermal capacity and delay in Table 4.

Cases A and B were also coincident in the optimal values of the windows infiltration rate ($10^{-5}$ kg/s/m, the lowest bound), the doors infiltration rate (0.02 kg/s/m, again the lowest bound), the type of roof (Level 5, the one with the lowest transmittance and the highest thermal capacity and delay in Table 4), the type of internal walls (Level 5, that with the highest thermal transmittance and capacity and the lowest delay in Table 4) and windows glazing (Level 4, the one having the lowest transmittance). General recommendations for building this type of house in Littoral can be easily derived from these common results for Cases A and B.

Also, results from Case B show more sensitiveness to local weather: Solar gains were favored through the

North-facing façade (large and medium-shaded windows, high external thermal absorptance) while they were controlled through East- and West-facing façades (narrow and well-shaded windows, low external solar absorptance).

### 3.4. Discussion on computational efficiency

A crucial feature of the current methodology is its parallel computing capability, taking advantage of the Pirayu cluster installed at our laboratory. This cluster has 600 Intel® Xeon® CPU E5-2650 v3 @ 2.30GHz cores. Using one of these cores, it took 2 to 2.5 minutes to run $E^+$ to determine the fitness of an individual. Now, using 64 of these cores in parallel, the fitness of the whole population was evaluated in approximately the same time. So, the optimal solutions of Case A (after 100 generations) and Case B (after 150 generations) took 4.5h to 6.6h, respectively. Let us note that, running in a sequential mode in an Intel® Core™ i7-5820K desktop PC, 12 days are needed to obtain the optimal solution for Case A, and more than 16 days for Case B. Using the current parallel tool running in the six cores of this PC a perfect speed-up can be obtained, i.e., the computational time is divided by 6 taking 2 days approximately. So, the current tool is also very efficient in regular multicore PCs.

## 4. Conclusions

In this work, a multi-objective optimization method to improve energy efficiency and thermal comfort in dwellings using a simulation-based optimization technique was proposed. The performance of the house was characterized by two normalized objectives taking into account different thermal zones and passive as well as active cooling and heating strategies. The set of more influent design variables were explored to find the optimal trade-off between cooling and heating performance.

As a result of the optimization, reductions were achieved not only in the normalized objectives but also in the sub-objectives: up to 95% fewer heating degree-hours and 99% fewer cooling degree-hours in the living room, and up to 99% less heating energy consumption and up to 82% less cooling energy in the bedrooms (taking as reference the same house as it was originally designed and built). This validated the efficiency and robustness of the routines developed that couple the NSGA-II with EnergyPlus for solving the current multi-objective optimization problem through a computing cluster implementation.

Regarding the current results for a typical house in the Argentine Littoral region, they served to dictate general recommendations for the design of dwellings in this region: external walls and roofs should have low thermal transmittance and high thermal capacity and high thermal delay, the internal ones should have high thermal transmittance and capacitance and low delay, the windows should have low transmittance, among others.

The parallel implementation in Pirayu cluster allowed to reduce the optimization time from more than a week in a sequential PC to a few hours. This will permit to apply this methodology to optimize a wide variety of building typologies in Argentina, and to do that in real-world times as it is required by the current critical situation of the electrical sector, which is our next goal. By the way, we also plan to make the current BPO tool, running in the clusters installed at our laboratory, accessible to general users via a web-platform interface.

Furthermore, in future works will be addressed to include important aspects of indoor environmental quality (visual and acoustic comfort, indoor air quality, etc.) as well as the impact of the climate change in the definition of the objective functions. We will also work on further reducing the computational time by both using meta-models for fitness evaluation and going deeper on the efficiency of optimization solvers.

## Acknowledgments

For funding this work, we would like to thank the Agency for Science, Technology and Innovation (SECTEI) of the Province of Santa Fe (Argentina) via the Research Project 2010-022-16 "Optimization of the Energy Efficiency of Buildings in the Province of Santa Fe", and from the National University of Littoral (Argentina) via the Project CAI+D 50120110100441LI "Saving energy for housing air-conditioning in the Argentinean Littoral region".

The present work uses the computational resources of the Pirayu group, acquired with Funds from the Santa Fe Province Agency of Science, Technology and Innovation (ASACTEI) of the Province of Santa Fe, through Project AC-00010-18, Resolution N° 117/14. This equipment is part of the National System of Computing in the High Performance of the Argentine Ministry of Science and Technology.

We would also like to thank Alejandro Dabin and Juan Pablo Dorsch for their help in the use of the Pirayu cluster.

F. Bre is a doctoral student granted by the National Scientific and Technical Research Council of Argentina (CONICET).

## References

[1] Boletín Oficial de la República Argentina [Argentine Official Gazzette]. Decreto 134/2015: Emergencia energética [Decrete 134/2015: Energy emergency] [in Spanish], December 17th, 2015. URL `https://www.boletinoficial.gob.ar/pdf/linkQR/Nnh0S05RRXhTRFUrdTVReEh2ZkU0dz09`.

[2] E. Apud, J. C. Aráoz, A. E. Devoto, R. E. Alieto, A. Guadagni, J. Lape na, D. G. Montamat, and R. A. Olocco (Former Argentine Secretaries of Energy). *CONSENSOS ENERGÉTICOS 2015 [ENERGY CONSENSUS 2015] [in Spanish]*. Instituto Argentino de la Energía General Mosconi, 2015.

[3] Ministerio de Energía y Minería de la República Argentina [Argentine Ministry of Energy and Mining]. Balance energético nacional - Año 2015 - Revisión 2 – Datos preliminares [National energy balance - Year 2015 - Revision 2 – Preliminary data] [in Spanish], 2014. URL `http://www.energia.gob.ar/contenidos/verpagina.php?idpagina=3366`.

[4] Instituto Argentino de Normalización y Certificación [Argentine Institute of Standards and Certification] (IRAM). IRAM 11900. Etiqueta de eficiencia energética de calefacción para edificios. Clasificación según la transmitancia térmica de la envolvente [Building heating energy efficiency label. Classification according to the thermal transmittance of the building envelope] [in Spanish], 2010.

[5] M. C. Peel, B. L. Finlayson, and T. A. McMahon. Updated world map of the Köppen-Geiger climate classification. *Hydrol. Earth Syst. Sci.*, 11:1633–1644, 2007.

[6] Instituto Argentino de Normalización y Certificación [Argentine Institute of Standards and Certification] (IRAM). IRAM 11603. Acondicionamiento térmico de edificios. Clasificación bioambiental de la República Argentina [Thermal conditioning of buildings. Bioenvironmental classification of Argentina] [in Spanish], 2012.

[7] Intergovernmental Panel on Climate Change (IPCC). *Climate Change 2014: Impacts, Adaptation, and Vulnerability. Part B: Regional Aspects. Contribution of Working Group II to the Fifth Assessment Report of the Intergovernmental Panel on Climate Change.* Cambridge University Press, 2014.

[8] A. Invidiata and E. Ghisi. Impact of climate change on heating and cooling energy demand in houses in Brazil. *Energy and Buildings*, 130:20–32, 2016.

[9] Y.-H. Lin, K.-T. Tsai, M.-D. Lin, and M.-D. Yang. Design optimization of office building envelope configurations for energy conservation. *Applied Energy*, 171:336–346, 2016.

[10] H. Islam, M. Jollands, S. Setunge, and M. A. Bhuiyan. Optimization approach of balancing life cycle cost and environmental impacts on residential building design. *Energy and Buildings*, 87:282–292, 2015.

[11] N. Delgarm, B. Sajadi, S. Delgarm, and F. Kowsary. A novel approach for the simulation-based optimization of the buildings energy consumption using NSGA-II: Case study in Iran. *Energy and Buildings*, 127:552–560, 2016.

[12] Y. Lu, S. Wang, Y. Zhao, and C. Yan. Renewable energy system optimization of low/zero energy buildings using single-objective and multi-objective optimization methods. *Energy and Buildings*, 89:61–75, 2015.

[13] W. Yu, B. Li, H. Jia, M. Zhang, and D. Wang. Application of multi-objective genetic algorithm to optimize energy efficiency and thermal comfort in building design. *Energy and Buildings*, 88:135–143, 2015.

[14] L. Magnier and F. Haghighat. Multiobjective optimization of building design using trnsys simulations, genetic algorithm, and artificial neural network. *Building and Environment*, 45(3):739–746, 2010.

[15] E. Asadi, M. G. da Silva, C. H. Antunes, L. Dias, and L. Glicksman. Multi-objective optimization for building retrofit: A model using genetic algorithm and artificial neural network and an application. *Energy and Buildings*, 81:444–456, 2014.

[16] R. V. Lenth. Some practical guidelines for effective sample size determination. *The American Statistician*, 55(3):187–193, August 2001.

[17] G. M. Mauro, M. Hamdy, G. P. Vanoli, N. Bianco, and J. L. M. Hensen. A new methodology for investigating the cost-optimality of energy retrofitting a building category. *Energy and Buildings*, 107:456–478, 2015.

[18] F. Ascione, N. Bianco, C. De Stasio, G. M. Mauro, and G. P. Vanoli. CASA, cost-optimal analysis by multi-objective optimisation and artificial neural networks: A new framework for the robust assessment of cost-optimal energy retrofit, feasible for any building. *Energy and Buildings*, 146:200–219, 2017.

[19] A. P. Melo, R. S. Versage, G. Sawaya, and R. Lamberts. A novel surrogate model to support building energy labelling system: A new approach to assess cooling energy demand in commercial buildings. *Energy and Buildings*, 131:233–247, 2016.

[20] F. Bre, A. S. Silva, E. Ghisi, and V. D. Fachinotti. Residential building design optimisation using sensitivity analysis and genetic algorithm. *Energy and Buildings*, 133:853–866, 2016.

[21] R. Garber. Optimisation stories: The impact of building information modelling on contemporary design practice. *Architectural Design*, 79(2):6–13, 2009.

[22] T. Méndez Echenagucia, A., Capozzoli, Y. Cascone, and M. Sassone. The early design stage of a building envelope: Multi-objective search through heating, cooling and lighting energy performance analysis. *Applied Energy*, 154:577–591, 2015.

[23] M. Fesanghary, S. Asadi, and Z. W. Geem. Design of low-emission and energy-efficient residential buildings using a multi-objective optimization algorithm. *Building and environment*, 49:245–250, 2012.

[24] V Pareto, Cours D'Economie Politique, and F Rouge. Lausanne. *Volume I and II*, 1896.

[25] Kaisa Miettinen. *Nonlinear Multiobjective Optimization*, volume 12. Kluwer Academic Publishers, Dordrecht, 1999.

[26] K. Deb. *Multi-objective optimization using evolutionary algorithms*, volume 16. John Wiley & Sons, 2001.

[27] C. Koo, T. Hong, M. Lee, and J. Kim. An integrated multi-objective optimization model for determining the optimal solution in implementing the rooftop photovoltaic system. *Renewable and Sustainable Energy Reviews*, 57:822–837, 2016.

[28] A. Konak, D. W. Coit, and A. E. Smith. Multi-objective optimization using genetic algorithms: A tutorial. *Reliability Engineering & System Safety*, 91(9):992–1007, 2006.

[29] R. Eberhart and J. Kennedy. A new optimizer using particle swarm theory. In *Micro Machine and Human Science, 1995. MHS'95., Proceedings of the Sixth International Symposium on*, pages 39–43. IEEE, 1995.

[30] E. Zitzler, M. Laumanns, L. Thiele, et al. Spea2: Improving the strength pareto evolutionary algorithm, 2001.

[31] K. Deb, A. Pratap, S. Agarwal, and T. Meyarivan. A fast and elitist multiobjective genetic algorithm: NSGA-II. *IEEE Transactions on Evolutionary Computation*, 6(2):182–197, 2002.

[32] M. Wetter and J. Wright. A comparison of deterministic and probabilistic optimization algorithms for nonsmooth simulation-based optimization. *Building and Environment*, 39(8):989–999, 2004.

[33] A.-T. Nguyen, S. Reiter, and P. Rigo. A review on simulation-based optimization methods applied to building performance analysis. *Applied Energy*, 113:1043–1058, 2014.

[34] M. Hamdy, A.-T. Nguyen, and J. L. M. Hensen. A performance comparison of multi-objective optimization algorithms for solving nearly-zero-energy-building design problems. *Energy and Buildings*, 121:57–71, 2016.

[35] S. Carlucci, G. Cattarin, F. Causone, and L. Pagliano. Multi-objective optimization of a nearly zero-energy building based on thermal and visual discomfort minimization using a non-dominated sorting genetic algorithm (NSGA-II). *Energy and Buildings*, 104:378–394, 2015.

[36] F. Ascione, R. F. De Masi, F. de Rossi, S. Ruggiero, and G. P. Vanoli. Optimization of building envelope design for nZEBs in Mediterranean climate: Performance analysis of residential case study. *Applied Energy*, 183:938–957, 2016.

[37] A. E. I. Brownlee and J. A. Wright. Constrained, mixed-integer and multi-objective optimisation ofbuilding designs by NSGA-II with fitness approximation. *Applied Soft Computing*, 33:114–126, 2015.

[38] M. Ehrgott and D. Tenfelde-Podehl. Computation of ideal and nadir values and implications for their use in mcdm methods. *European Journal of Operational Research*, 151(1):119–139, 2003.

[39] D. B. Crawley, L. K. Lawrie, F. C. Winkelmann, W. F. Buhl, Y. J. Huang, C. O. Pedersen, R. K. Strand, R. J. Liesen, D. E Fisher, M. J. Witte, and J. Glazer. EnergyPlus: creating a new-generation building energy simulation program. *Energy and buildings*, 33(4):319–331, 2001.

[40] F.-A. Fortin, F.-M. De Rainville, M.-A. Gardner, M. Parizeau, and C. Gagné. DEAP: Evolutionary algorithms made easy. *Journal of Machine Learning Research*, 13:2171–2175, july 2012.

[41] F.-A. Fortin and M. Parizeau. Revisiting the nsga-ii crowding-distance computation. In *Proceedings of the 15th annual conference on Genetic and evolutionary computation*, pages 623–630. ACM, 2013.

[42] K. Deep, K. P. Singh, M. L. Kansal, and C. Mohan. A real coded genetic algorithm for solving integer and mixed integer optimization problems. *Applied Mathematics and Computation*, 212(2):505–518, 2009.

[43] D. E. Goldberg and J. H. Holland. Genetic algorithms and machine learning. *Machine learning*, 3(2):95–99, 1988.

[44] V. Vanovschi. Parallel python software, 2016. URL `http://www.parallelpython.com`.

[45] CIMEC. Cluster Pirayu. URL `http://www.cimec.org.ar/c3/pirayu/`.

[46] Administración Nacional de la Seguridad Social de la República Argentina [Argentine Social Security Administration] (ANSES). Programa de Crédito Argentino [Argentine Loans Programme] (PROCREAR) [in Spanish], 2016. URL `http://www.procrear.anses.gob.ar/`.

[47] F. Bre and V. D. Fachinotti. Generation of typical meteorological years for the Argentine Littoral region. *Energy and Buildings*, 129:432–444, 2016.

[48] D. B. Crawley and L. K. Lawrie. Climate.OneBuilding.Org. URL `http://climate.onebuilding.org`.

[49] National Renewable Energy Laboratory (NREL). Weather Data Sources, 2017. URL `https://energyplus.net/weather/sources`.

[50] Simulation Research Group at Lawrence Berkeley National Laboratory, Building Systems Laboratory at University of Illinois Urbana-Champaign, and other authors. EnergyPlus™ Documentation, v8.4.0 – Engineering Reference, 2015. URL `https://energyplus.net/documentation`.

[51] U.S. Department of Energy (DoE). *EnergyPlus, Input Output Reference – The Encyclopedic Reference to EnergyPlus Input and Output*, 2012.

[52] American Society of Heating, Refrigerating and Air-Conditioning Engineers (ASHRAE). *2009 ASHRAE® Handbook – Fundamentals.* Atlanta, Georgia, USA, 2009.

[53] American National Standards Institute (ANSI) and American Society of Heating, Refrigerating and Air-Conditioning Engineers (ASHRAE). *ANSI/ASHRAE Standard 55-2013. Thermal Environmental Conditions for Human Occupancy*, 2013.

[54] M. D. Morris. Factorial sampling plans for preliminary computational experiments. *Technometrics*, 33(2): 161–174, 1991.

# Highlights

- A method for the multi-objective optimization of residential buildings, taking advantage of high performance computing, was introduced.
- An actual single-family, two-story house in the Argentine Littoral region was the case study.
- The normalized degree-hours and the energy consumption in a separate way for winter and summer were the objective functions.
- The thermal and energy performance of the case study was drastically improved.